BJP BRITISH JOURNAL OF PHARMACOLOGY
BPS BRITISH PHARMACOLOGICAL SOCIETY

BJP British Journal of Pharmacology

DOI:10.1111/j.1476-5381.2010.00946.x
www.brjpharmacol.org

RESEARCH PAPER

Participation of CYP2C8 and CYP3A4 in the N-demethylation of imatinib in human hepatic microsomes

Correspondence
Dr Michael Murray, Faculty of Pharmacy, University of Sydney, NSW 2006, Australia. E-mail: michaelm@pharm.usyd.edu.au

Keywords
imatinib N-demethylation; CYP2C8; CYP3A4; human liver

Received
7 March 2010
Revised
9 May 2010
Accepted
7 June 2010

Noelia Nebot[1], Severine Crettol[1], Fabrizio d'Esposito[1], Bruce Tattam[2], David E Hibbs[3] and Michael Murray[1]

[1]*Pharmacogenomics and Drug Development Group, Faculty of Pharmacy, University of Sydney, NSW, Australia,* [2]*Thomas R Watson Mass Spectrometry Facility, Faculty of Pharmacy, University of Sydney, NSW, Australia and* [3]*Pharmaceutical Chemistry, Faculty of Pharmacy, University of Sydney, NSW, Australia*

BACKGROUND AND PURPOSE

Imatinib is a clinically important inhibitor of tyrosine kinases that are dysregulated in chronic myelogenous leukaemia and gastrointestinal stromal tumours. Inter-individual variation in imatinib pharmacokinetics is extensive, and influences drug safety and efficacy. Hepatic cytochrome P450 (CYP) 3A4 has been implicated in imatinib N-demethylation, but the clearance of imatinib decreases during prolonged therapy. CYP3A phenotype correlates with imatinib clearance at the commencement of therapy, but not at steady state. The present study evaluated the possibility that multiple CYPs may contribute to imatinib oxidation in liver.

EXPERIMENTAL APPROACH

Imatinib biotransformation in human liver microsomes (n = 20) and by cDNA-expressed CYPs was determined by LC–MS. Relationships between imatinib N-demethylation and other drug metabolizing CYPs were assessed.

KEY RESULTS

N-desmethylimatinib formation was correlated with microsomal oxidation of the CYP3A4 substrates testosterone (ρ = 0.60; P < 0.01) and midazolam (ρ = 0.46; P < 0.05), and the CYP2C8 substrate paclitaxel (ρ = 0.58; P < 0.01). cDNA-derived CYPs 2C8, 3A4, 3A5 and 3A7 supported imatinib N-demethylation, but 10 other CYPs were inactive; in kinetic studies, CYP2C8 was a high-affinity enzyme with a catalytic efficiency ~15-fold greater than those of CYPs 3A4 and 3A5. The CYP3A inhibitors ketoconazole and troleandomycin, and the CYP2C8 inhibitors quercetin and paclitaxel decreased imatinib oxidation. From molecular modelling, the imatinib structure could be superimposed on a pharmacophore for CYP2C8 substrates.

CONCLUSIONS AND IMPLICATIONS

CYP2C8 and CYPs 3A contribute to imatinib N-demethylation in human liver. The involvement of CYP2C8 may account in part for the wide inter-patient variation in imatinib pharmacokinetics observed in clinical practice.

Abbreviations

CYP, cytochrome P450; f_u, fraction unbound; LC–MS/MS, liquid chromatography–tandem mass spectrometry

Introduction

Imatinib mesylate (Gleevec) is the prototype of a new class of oncology drugs that target tyrosine kinases that are dysregulated in chronic myelogenous leukaemia and gastrointestinal stromal tumors (Druker *et al.*, 1996; Demetri *et al.*, 2002). In contrast to more established cytotoxic drugs that are administered according to cycles that are separated by drug-free recovery periods, treatment with imatinib is continous. Although the drug is generally well tolerated, adverse events in some patients are

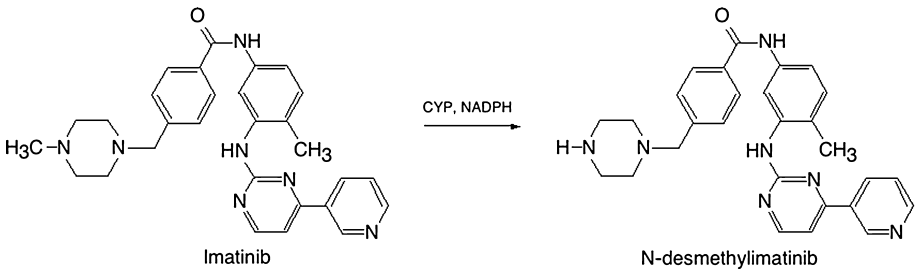

Figure 1
CYP-dependent oxidation of imatinib to N-desmethylimatinib.

severe and include the hand–foot syndrome, hepatotoxicity and cardiotoxicity (Guilhot, 2004; Ayoub *et al.*, 2005; Kerkela *et al.*, 2006). The development of drug resistance with imatinib is also significant and has been associated with the emergence of new clonal populations of tumour cells carrying additional oncogenic mutations (Deininger, 2008). However, pharmacokinetic mechanisms, such as the failure to maintain effective therapeutic concentrations of the drug in serum, may also contribute to imatinib resistance (Apperley, 2007; Blasdel *et al.*, 2007; Goldman, 2007). Moreover, pharmacokinetic–pharmacodynamic relationships have been established recently for imatinib, thereby justifying the use of serum concentration data in deciding patient dosage (Delbaldo *et al.*, 2006; Picard *et al.*, 2007).

The pharmacokinetic elimination of imatinib is subject to extensive inter-individual variation, and dose adjustment is achieved by trial and error after therapy has commenced. Dose optimization based on both drug pharmacokinetics and pharmacogenetic variation in the pathways of imatinib biotransformation may enhance the safety and efficacy of imatinib therapy in patients. Imatinib is metabolized primarily by hepatic oxidation to N-desmethylimatinib (or CGP74588; Figure 1), which is also pharmacologically active (Peng *et al.*, 2005). An important role for cytochrome P450 (CYP) 3A (nomenclature follows Alexander *et al.*, 2009) in this pathway is supported by clinical findings, including drug interactions with other CYP substrates and inducers (Peng *et al.*, 2002; O'Brien *et al.*, 2003; Bolton *et al.*, 2004; Dutreix *et al.*, 2004; van Erp *et al.*, 2007). Moreover, *in vivo* CYP3A phenotype, as reflected by the clearance of the CYP3A substrates erythromycin and midazolam, was correlated with imatinib clearance at the commencement of therapy (Gurney *et al.*, 2007). However, at steady state (day 28 of therapy), imatinib clearance was no longer correlated with CYP3A phenotype. In view of the reported capacity of imatinib to inhibit CYP3A (O'Brien *et al.*, 2003) and the accumulation of imatinib during therapy (Gurney *et al.*, 2007), it is possible that other CYPs may contribute to imatinib N-demethylation; this may also be responsible in part for the observed inter-individual differences in efficacy and toxicity of the drug (Peng *et al.*, 2005; Gardner *et al.*, 2006). The present study evaluated the participation of a range of CYPs in imatinib N-demethylation in human liver. From a series of approaches including estimation of metabolite formation in human liver microsomes and cDNA-expressed CYPs, as well as the use of pharmacological inhibitors of specific CYPs, the principal finding to emerge was that CYP2C8 and CYP3A mediate the oxidation of imatinib in human samples.

Methods

Liver donors and preparation of microsomal fractions

The present study was approved by institutional ethics committees in accordance with the Declaration of Helsinki. Human liver was obtained as surplus material during orthotopic transplantation or from biopsies from the normal margin during liver resection (Queensland and Australian Liver Transplant Programs, Princess Alexandria Hospital, Brisbane, Queensland, and Royal Prince Alfred Hospital, Sydney, NSW, Australia, respectively). Tissue was perfused with Viaspan solution at 4°C (DuPont, Wilmington, DE, USA), and transported to the laboratory on ice. Hepatic microsomes were prepared (Murray *et al.*, 1983) and microsomal protein was determined as described previously (Lowry *et al.*, 1951).

Liquid chromatography–tandem mass spectrometry (LC–MS/MS) analysis of imatinib N-demethylation by human CYPs

LC–MS/MS was used to quantify imatinib N-demethylation. Separation was achieved on a Hewlett Packard 1090 Liquid Chromatograph (Palo Alto, CA, USA) using an Altima C18 5μ column

(150 × 2.1 mm i.d.; Alltech Associates, Castle Hill, NSW, Australia). The mobile phase was 90% aqueous methanol containing 0.5% ammonium acetate at a flow rate of 0.3 mL·min^{-1}. The LC–MS interface (Finnigan MAT TSQ 7000 system; San Jose, CA, USA) used electrospray ionization operating in positive ionization mode with high-purity nitrogen (BOC, Sydney, NSW, Australia) as the sheath gas at 80 psi, and ultra-high-purity argon (BOC) as the collisional gas at 2.2 mtorr. The spray current was 4.5 kV and the temperature of the heated capillary was 275°C, with selected reaction monitoring for quantification of the ion transitions of 494.1 to 394.1 for imatinib, 480.2 to 394.1 for N-desmethylimatinib and 502.2 to 394.1 for imatinib-d8. Collision energies of 28 eV were used for imatinib and its metabolite, and 30 eV for imatinib-d8. Xcalibur 1.2 Core Data Software and Finnigan XSQ MS 1.1 instrument software were used in data acquisition and analysis.

Varian Bond Elut Plexa solid-phase extraction cartridges (1 mL, Varian Australia Pty Ltd, Mulgrave, Victoria, Australia) were used for isolation of imatinib and its N-desmethyl metabolite in conjunction with a Gilson ASPEC XL4 solid-phase instrument (Villiers-le-Bel, France) under the control of 735 Sampler software package version 6.0 (Solassol *et al.*, 2006). Cartridges were preconditioned with methanol (1.25 mL × 2) and water (1.25 mL × 2), and then the samples (0.5 mL) were loaded and washed with 5% aqueous methanol (2 × 2 mL aliquots) prior to elution with methanol (3 × 1.25 mL aliquots). Possible matrix effects were assessed by adding authentic standards to blank microsomal fractions. Calibration curves were constructed for imatinib that had been extracted from microsomal fractions using six different concentrations in triplicate over the range 100–5000 ng·mL^{-1}. In addition, replicate concentrations (50, 100, 1000 ng·mL^{-1}) were analysed in six different human liver microsomal samples. Intra- and inter-day precision and accuracy for imatinib and N-desmethylimatinib were estimated on three separate days.

Imatinib biotransformation in microsomal fractions

Incubation mixtures (0.2 mL) contained imatinib (80 μM), microsomal protein (150 μg) and NADPH (2 mM) in potassium phosphate buffer (0.1 M, pH 7.4). Reactions were run at 37°C for 10 min, and were terminated with 5% trifluoroacetic acid (5 μL). Imatinib N-demethylation in human hepatic microsomes was linear under these conditions. In kinetic studies, imatinib N-demethylation was determined over the substrate range 5–200 μM.

The activities of cDNA-expressed CYPs (10 pmol) in imatinib N-demethylation were determined at a substrate concentration of 20 μM, except in kinetic studies where the concentration range was 5–300 μM, in potassium phosphate buffer (0.1 M, pH 7.4). Although the specific contents of these systems determined by the manufacturer (pmol CYP·mg protein^{-1}) varied somewhat, the experimental data were scaled to pmol·CYP^{-1}, as proposed by Crespi and Penman (1997). Reactions were initiated with 1 mM NADPH, and terminated after 60 min with 5% trifluoroacetic acid and removal to ice. N-desmethylimatinib was quantified as described above.

Other microsomal assays of CYP-dependent substrate oxidation

CYP2B6-dependent bupropion hydroxylation was determined essentially as described previously (Loboz *et al.*, 2005), with minor modifications. Briefly, incubations (37°C, 20 min) contained microsomal protein (0.15 mg) and bupropion (500 μM) in potassium phosphate buffer (0.1 M, pH 7.4), and were initiated with 1 mM NADPH. Reactions were terminated with cold acetonitrile (0.8 mL) and centrifuged at 10 000× *g* for 15 min. The organic layer was evaporated under a stream of nitrogen and reconstituted in mobile phase (methanol : phosphate buffer (0.05 M, pH 5.5, 65:35) for analysis by HPLC (Loboz *et al.*, 2005). Chromatography was conducted on a Synergi Polar-RP column, 250 × 4.6 mm i.d., 4 μ particle size (Phenomenex, Lane Cove, NSW, Australia) at a flow rate of 0.6 mL·min^{-1}. The retention times of bupropion, hydroxybupropion and the internal standard timolol were 16.4, 10.6 and 9.3 min respectively. Detection was by dual wavelength diode array at 254 nm for bupropion and timolol, and 214 nm for hydroxybupropion.

CYP2C8-mediated paclitaxel 6α-hydroxylation activity was determined by an adaptation of previous methods (Vaclavikova *et al.*, 2003). Incubations (37°C, 90 min) contained microsomal protein (0.15 mg) and paclitaxel (25 μM) in potassium phosphate buffer (0.1 M, pH 7.4), and were initiated with 1 mM NADPH. Reactions were terminated with cold acetonitrile (1 mL) and centrifuged at 10 000× *g* for 15 min. The organic layer was evaporated under a stream of nitrogen, reconstituted with 0.1 mL mobile phase (20 mM ammonium acetate : acetonitrile : methanol; 5:3:2) and subjected to HPLC analysis on a Finepak SIL C18-5 column (15 cm × 4.6 mm i.d.; JASCO, Meadowbank, NSW, Australia) at a flow rate of 1 mL·min^{-1} with UV detection at 227 nm. Retention times for timolol, 6α-hydroxypaclitaxel and paclitaxel were 8.6, 13 and 19 min respectively.

CYP2A6-dependent coumarin 7-hydroxylation was estimated by the method by Miles *et al.* (1990). Reactions contained microsomal protein (40 μg)

and coumarin (50 μM) in 0.1 M Tris–chloride buffer, pH 7.4 (0.2 mL), and were initiated with 0.75 mM NADPH. After 15 min, reactions were stopped with 6% aqueous trichloroacetic acid, centrifuged at 14 000× *g* for 10 min, and the supernatant (0.5 mL) was mixed with 3 mL 0.8 M Tris–glycine, pH 9. Product formation was determined in a FLUOstar Optima microplate reader (BMG Labtech, Offenburg, Germany) with emission and excitation wavelengths set at 460 and 376 nm respectively.

Other microsomal assays were conducted as follows: testosterone 6β-hydroxylation (mediated by CYP3A) (Murray, 1992), dextromethorphan O-demethylation (CYP2D6) (Zhang *et al.*, 2008), 7-ethoxyresorufin *O*-deethylation (CYP1A2) (Zhang *et al.*, 2008), *N*,*N*-dimethylnitrosamine N-demethylation (CYP2E1) (Murray *et al.*, 1994), lauric acid 12-hydroxylation (CYP4A11) (Su *et al.*, 2005), midazolam 1′-hydroxylation (CYP3A) (Zhang *et al.*, 2008) and tolbutamide 4-hydroxylation (CYP2C9) (Murray *et al.*, 1994). The unbound fraction (f_u) of imatinib in microsomal fractions was determined in Microcon YM-10 devices (10 kDa molecular weight cut-off; Millipore Corp., Bedford, MA, USA) using 80 μM imatinib and 150 μg microsomal protein, as described by Zhang *et al.* (2007).

Computational methods

All molecules investigated in this study were built with the molecular modelling and graphical user interface package, Maestro 9.0, unless otherwise stated. Each structure was subsequently minimized using the OPLS_2005 forcefield with a constant dielectric of 1.0. All calculations were performed on an Intel Xeon workstation using the SUSE11.1 Linux operating system.

Pharmacophore preparation was carried out using PHASE 3.0 in the Maestro modelling environment. A maximum of 100 conformations was generated for imatinib, sampling the torsional space that may contain possible active conformers. This was achieved using a combination of Monte Carlo Minimum and low-mode conformational searching, in conjugation with the OPLS_2005 force field, GB/SA solvation treatment and a minimum atom deviation of 1.0 Å. This was conducted to exhaustively search all conformational space in a water-solvated environment. Minimized structures were filtered with a maximum relative energy difference of 10.0 kcal·mol^{-1} to exclude redundant conformers.

Statistical analyses

Data are expressed throughout as means ± SEM. CYP activities were estimated in individual human hepatic fractions and cDNA-expressed systems in incubations at least in duplicate. Initial Shapiro–Wilk testing established that the hepatic microsomal data were not normally distributed. Differences between sample groups were detected with the Mann–Whitney *U*-test, and subsequent non-parametric statistical analyses were performed (Statview; Abacus Concepts, Berkeley, CA, USA). Kinetic analysis was performed with GraphPad Prism (GraphPad Software Inc., La Jolla, CA, USA).

Materials

Imatinib mesylate, N-desmethylimatinib and imatinib-d8 (internal standard) were gifts from Novartis (Basel, Switzerland). [^{14}C]-Testosterone (specific activity: 57–59 mCi·mmol^{-1}), Hyper Film-MP and ASC-II scintillant were purchased from PerkinElmer (Rowville, VIC, Australia). Bupropion hydrochloride and hydroxybupropion were gifts from GlaxoSmithKline (Ermington, NSW, Australia). 6β-Hydroxypaclitaxel and 1′-hydroxymidazolam were purchased from Toronto Research Chemicals Inc. (North York, ON, Canada). All other CYP substrates, metabolites and inhibitors, as well as all biochemicals, were purchased from Sigma Aldrich (Castle Hill, NSW, Australia). Analytical reagent grade and HPLC grade solvents were from Lomb Scientific (Sydney, NSW, Australia). Silica gel 60 F254 plates for thin-layer chromatography were from Crown Scientific (Moorebank, NSW, Australia). cDNA-derived human CYPs expressed in human lymphoblastoid cell lines (CYPs 1A1, 1A2, 2C9, 2C19, 2D6, 2E1 and 3A4; for CYP3A4, the specific content was 42 pmol·mg protein^{-1}) and insect cell microsomes (CYPs 1B1, 2A6, 2B6, 2C8, 3A5, 3A7 and 4A11; for CYPs 2C8, 3A5 and 3A7, the specific contents were 400, 250 and 180 pmol·mg protein^{-1}, respectively) were obtained from Gentest Corp. (Woburn, MA, USA). Control microsomes were prepared from cells that had been transfected with blank expression vector alone.

Results

Microsomal CYP-dependent imatinib N-demethylation in human liver

An LC–MS/MS assay was developed for use in the characterization of imatinib N-demethylation by human CYPs; a representative chromatogram for the analysis is shown in Figure 2. By solid-phase extraction, the recovery of imatinib was 84–113% (CV < 10%), and N-desmethylimatinib was 78–83% (CV ≤ 5%); using solid-phase extraction prevented matrix effects. Calibration curves for extracted imatinib were linear (r^2 > 0.999) over the range 100–5000 ng·mL^{-1}. The intra- and inter-day precision and accuracy for imatinib and N-desmethylimatinib were

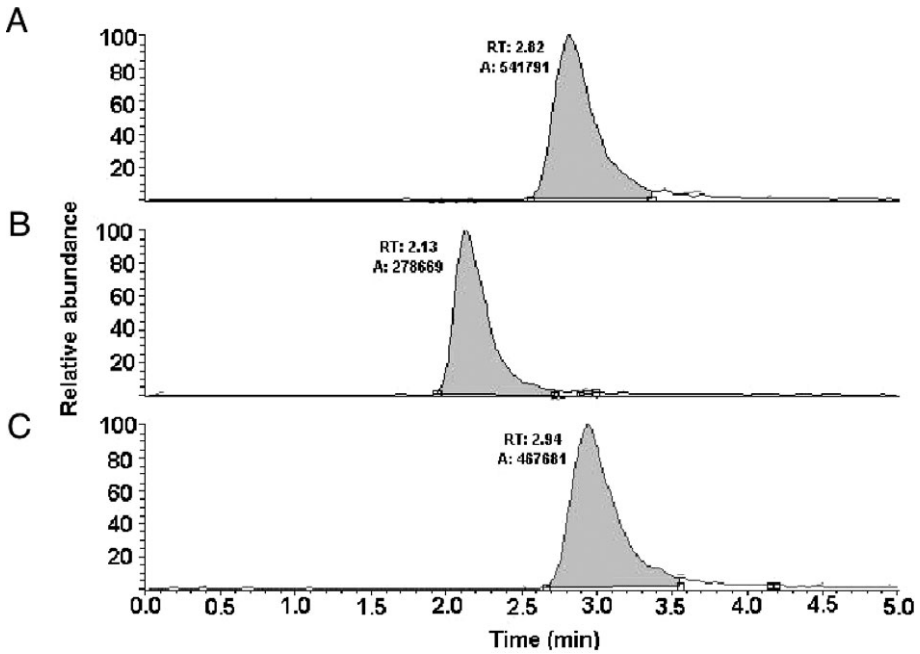

Figure 2

LC–MS/MS traces of (A) imatinib, (B) N-desmethylimatinib and (C) imatinib-d8 (internal standard) following solid-phase extraction of a human sample that had the authentic analytes added (as described in Methods).

estimated. Coefficients of variation for these parameters were in the range 0–13% of the nominal concentration in all cases (the acceptable limit is 15%), and the limit of quantitation was 50 ng·mL^{-1}. In separate studies, the f_u for imatinib in microsomal fractions was estimated by ultrafiltration to be 6.2%.

Twenty individual microsomal fractions were available for the present study. Median N-desmethylimatinib formation was 21 pmol·mg protein^{-1}·min^{-1}, and the range was 15–65 pmol·mg protein^{-1}·min^{-1} (Table 1). As shown in Figure 3, the formation of N-desmethylimatinib was correlated with CYP3A-mediated testosterone 6β-hydroxylation (Spearman's correlation coefficient $\rho = 0.60$, $P < 0.01$; Figure 3A) and midazolam 1′-hydroxylation ($\rho = 0.46$, $P < 0.05$; Figure 3B), as well as CYP2C8-mediated paclitaxel 6α-hydroxylation ($\rho = 0.58$, $P < 0.01$; Figure 3C) and CYP2C9-dependent tolbutamide 4-hydroxylation ($\rho = 0.57$, $P < 0.01$), but not with oxidation of dextromethorphan (CYP2D6), coumarin (CYP2A6), bupropion (CYP2B6), resorufin (CYP1A2), *N*,*N*-dimethylnitrosamine (CYP2E1) or lauric acid (CYP4A11) (not shown). In these samples, paclitaxel 6α-hydroxylation was not significantly correlated with testosterone 6β-hydroxylation ($\rho = 0.38$, $P = 0.10$) or midazolam 1′-hydroxylation ($\rho = 0.22$, $P = 0.36$).

In kinetic studies, imatinib N-demethylation was estimated at a range of substrate concentrations (5–200 μM). From non-linear regression, the apparent K_m range in five individual microsomal fractions was 22–55 μM, and the V_{max} was 85–175 pmol N-desmethylimatinib·mg protein^{-1}·min^{-1} with catalytic efficiencies (V_{max}/K_m) in the range 2.0–6.7 pmol N-desmethylimatinib·mg protein^{-1}·min^{-1}·μM^{-1} (GraphPad Prism 5). A representative kinetic analysis undertaken in HL42 microsomes is shown in Figure 4A.

Metabolism of imatinib by individual cDNA-derived human CYPs

As shown in Figure 4B, cDNA-derived CYPs 2C8, 3A4, 3A5 and to a lesser extent 3A7 catalysed imatinib N-demethylation (155, 83, 66 and 22 pmol product·pmol CYP^{-1}·h^{-1}, respectively), but CYPs 1A1, 1A2, 1B1, 2A6, 2B6, 2C9, 2C19, 2D6, 2E1 and 4A11 were essentially inactive (Figure 4B). Kinetic parameters for imatinib N-demethylation by cDNA-derived CYP2C8, CYP3A4 and CYP3A5 were determined over an imatinib concentration range of 5–300 μM (Figure 4C). The apparent K_m for CYP2C8 was 1.4 μM, which was over an order of magnitude lower than those for CYP3A4 and CYP3A5 (44 and 43 μM respectively). The V_{max} values for CYPs 2C8, 3A4 and 3A5 were 24.5, 52.5 and 44.1 pmol product·pmol CYP^{-1}·h^{-1}, respectively, which give

Table 1
Individual variation in oxidation of imatinib and CYP-specific substrates in human hepatic microsomes

Liver sample	Medications of donor	Imatinib N-demethylation pmol·mg protein^{-1}·min^{-1}	Midazolam 1′-hydroxylation pmol·mg protein^{-1}·min^{-1}	Paclitaxel 6α-hydroxylation pmol·mg protein^{-1}·min^{-1}	Testosterone 6β-hydroxylation nmol·mg protein^{-1}·min^{-1}
HL4	None	24	0.45	27	3.33
HL16	Dopamine, desmopressin	29	1.07	32	1.42
HL17*	Bismuth subnitrate, sucralphate	20	1.03	61	0.12
HL19	None	24	0.3	62	1.07
HL21	Unknown	22	1.03	22	0.39
HL24	flucloxacillin, ceftriaxone	65	4.31	19	2.4
HL26	Dopamine, imipenem	35	3.06	54	0.95
HL28	Unknown	20	0.06	10	0.12
HL29	Simvastatin	32	1.73	96	2.17
HL30	Adrenaline, ranitidine, penicillin	16	0.91	21	0.26
HL31*	Dexamethasone, dopamine, desmopressin	30	0.79	68	0.83
HL35*	Dopamine	18	0.37	25	0.23
HL36	Unknown	18	0.67	16	0.68
HL42	Unknown	21	0.3	23	0.4
HL43	Unknown	33	1.3	49	1.04
HL45	Unknown	15	0.34	22	0.93
HL46	Unknown	17	1.08	14	0.93
HL47	Unknown	15	0.31	19	0.23
HL48	Unknown	16	0.62	22	0.78
HL49	Unknown	20	0.5	37	0.98
Median		21	0.73	24	0.88
Range		(15–65)	(0.06–4.31)	(10–96)	(0.12–3.33)

Data were derived in at least duplicate incubations that varied by <8% from the stated mean values.
*Smoker.

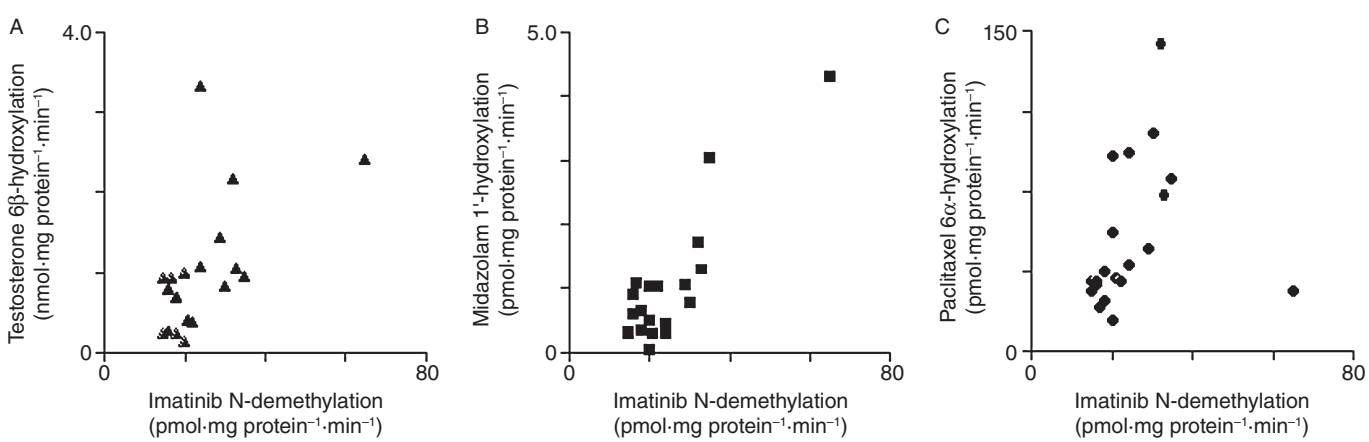

Figure 3
Linear relationships between microsomal imatinib N-demethylation and (A) CYP3A-dependent testosterone 6β-hydroxylation, (B) CYP3A-dependent midazolam 1′-hydroxylation and (C) CYP2C8-dependent paclitaxel 6α-hydroxylation.

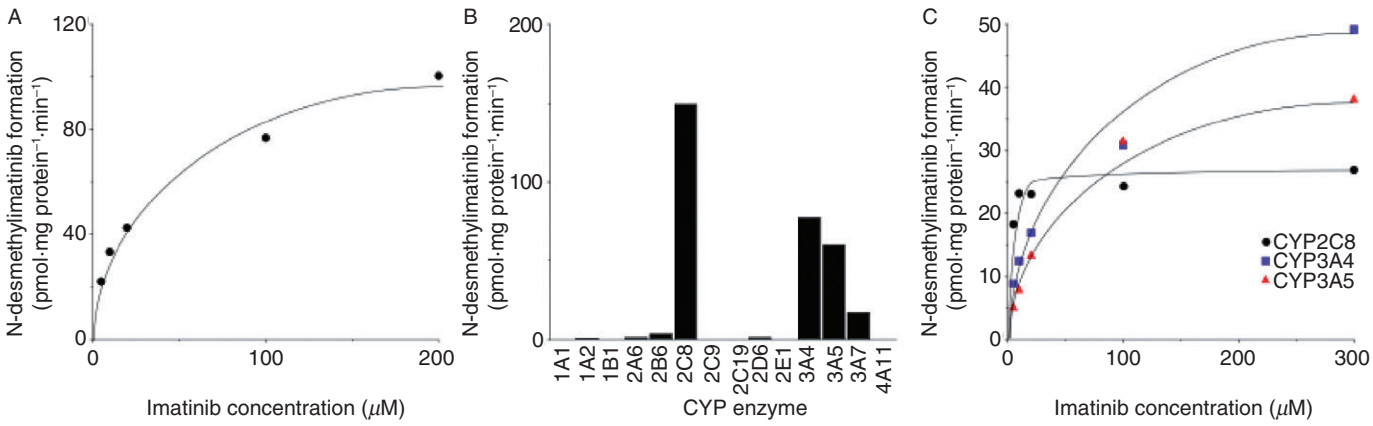

Figure 4

(A) Representative kinetic analysis of hepatic microsomal imatinib N-demethylation in HL42, (B) imatinib N-demethylation mediated by cDNA-expressed CYPs and (C) kinetic analysis of imatinib N-demethylation mediated by cDNA-expressed CYP2C8, CYP3A4 and CYP3A5. Data were derived in at least duplicate incubations that varied by <8% from the stated mean values.

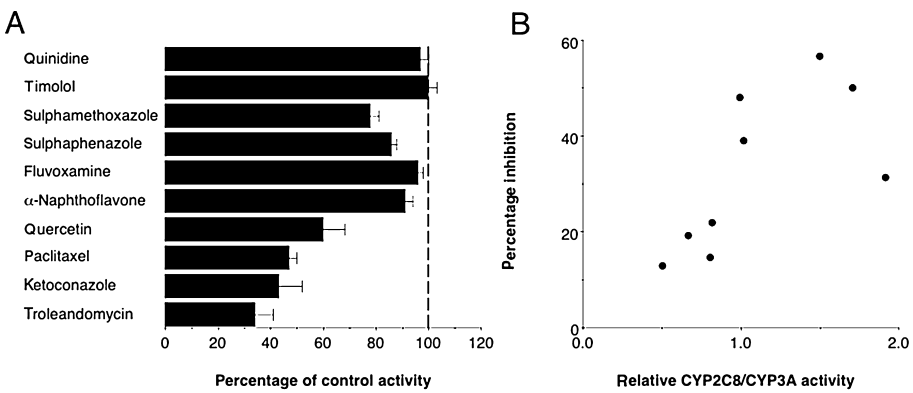

Figure 5

(A) Effects of CYP-specific inhibitors on imatinib N-demethylation (mean ± SEM in $n = 3$ individual hepatic microsomes), and (B) relationship between relative microsomal CYP2C8/CYP3A4 activities and susceptibility to inhibition by the CYP2C8 inhibitor quercetin (20 μM; $n = 9$ individual microsomal fractions).

rise to catalytic efficiency values for CYP2C8 (V_{max}/K_m = 17.5 pmol product·pmol CYP^{-1}·h^{-1}·μM^{-1}), CYP3A4 (V_{max}/K_m = 1.2 pmol product·pmol CYP^{-1}·h^{-1}·μM^{-1}) and CYP3A5 (V_{max}/K_m = 1.0 pmol product·pmol CYP^{-1}·h^{-1}·μM^{-1}). These findings suggest that CYP2C8 is about 15-fold more efficient than CYP3A4 and CYP3A5 in imatinib N-demethylation.

Modulation of imatinib N-demethylation by substrates and inhibitors of CYPs

The contributions of CYPs to imatinib N-demethylation were evaluated further using CYP-specific inhibitors. Inhibition was most extensive when human hepatic microsomes (HL4, HL17, HL47; Table 1) were incubated with the CYP3A inhibitors troleandomycin (250 μM; 24–47% of control activity in the absence of inhibitors) and ketoconazole (2 μM; 28–58% of control; Figure 5A). Significant inhibition was also observed with agents that modulate CYP2C8 activity, including quercetin (20 μM; 49–76% of control activity in the absence of inhibitors) and paclitaxel (45 μM; 42–54% of control). Indeed, further analysis undertaken in nine individual microsomal fractions revealed a relationship between relative CYP2C8/CYP3A activity and the susceptibility of imatinib N-demethylation to the CYP2C8 inhibitor quercetin (ρ = 0.78, $P < 0.02$; Figure 5B). In contrast, and as shown in Figure 5A, minimal inhibition of microsomal imatinib N-demethylation was produced by inhibitors of CYP2C9 (sulphaphenazole, 10 μM and sulphamethoxazole, 500 μM), CYP1A2 (α-naphthoflavone, 10 μM and fluvoxamine, 10 μM) and CYP2D6 (quinidine, 5 μM and timolol, 250 μM).

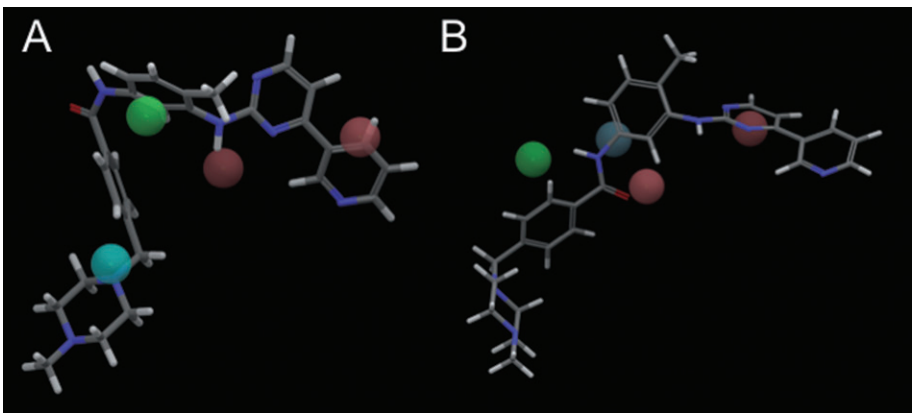

Figure 6

Structure of imatinib fitted to (A) the CYP2C8 and (B) the CYP3A4 pharmacophore models reported by Melet *et al.* (2004) and Ekins *et al.* (1999) respectively. Shown are hydrophobic regions (green sphere), polar groups (blue sphere) and hydrogen bond acceptors (red sphere).

Modelling

Pharmacophore models were created using a single reference structure, that of imatinib, and using an automated procedure, in which common pharmacophoric groups were exhaustively perceived among a set of low-energy relatives produced from a conformational search of all rotable bonds within imatinib. The hypotheses were then scored according to various geometric and heuristic criteria, yielding the top-ranked pharmacophore hypothesis. This scoring procedure returned an RMSD for the CYP2C8 hypothesis between collective conformers and pharmacophoric groups of less than 0.6 Å. Thus, imatinib fitted the proposed CYP2C8 pharmacophore well for features that included the polar group (blue sphere; Figure 6) and the hydrophobic/ring (green sphere), while the hydrogen bond acceptors (red spheres) for the amine and the pyridine were less well fitted. In contrast, the reported pharmacophore model for CYP3A4 did not fit imatinib functionalities particularly well, with the exception of the carbonyl H-bond acceptor; the alignment of the H-bond acceptor (red sphere) with the pyrimidine nitrogen in imatinib is an artefact arising from modification of the orientation to enhance clarity.

Discussion and conclusions

The present investigation has demonstrated that CYPs 3A (Ensembl ID ENSG00000160868 and ENSG00000106258 for CYPs 3A4 and 3A5, respectively; Alexander *et al.*, 2009) and 2C8 (Ensembl ID ENSG00000138115) participate in the oxidative N-demethylation of imatinib in human liver. These findings arose from experiments with cDNA-expressed CYPs, correlation of N-desmethylimatinib formation with rates of microsomal oxidation of substrates for CYP3A (testosterone and midazolam) and CYP2C8 (paclitaxel) and the inhibition of microsomal N-desmethylimatinib formation by the CYP3A4-specific inhibitors troleandomycin and ketoconazole, and the CYP2C8-specific inhibitors, quercetin and paclitaxel. Inhibitors of other CYPs were inactive.

The catalytic efficiency of CYP2C8 in imatinib N-demethylation was ~14.6 relative to CYP3A4 (calculated from the V_{max}/K_m ratios for the enzymes, 17.5/1.2; Figure 4C). Further, because CYP3A protein constitutes ~30% of total CYP in human liver compared to only ~7% for CYP2C8 (Shimada *et al.*, 1994), the relative contribution of CYP2C8 to overall hepatic imatinib N-demethylation at lower serum concentrations of the drug may be closer to ~3.4-fold that of CYP3A4 ($14.6 \times 7/30$). During standard therapy with imatinib (400 mg daily), the reported maximal serum concentration of the drug is ~4 μM, which can increase to at least twofold higher at elevated doses (Peng *et al.*, 2005). Although the intrahepatic concentration of imatinib during therapy may exceed that in serum, CYP2C8 is likely to be saturated at lower concentrations (K_m ~1.4 μM), while CYPs 3A retain residual capacity (K_m ~43 μM) that may contribute more significantly at higher concentrations.

Certain co-administered drugs and herbal agents are inducers of the hepatic expression of CYPs 3A *in vivo* (Sueyoshi and Negishi, 2001). Thus, in many cancer patients who receive concurrent therapy with other drugs, CYPs 3A may be induced and may contribute significantly to imatinib N-demethylation in human liver. Indeed, this is consistent with previous experimental and clinical reports in which imatinib was co-administered with drugs that inhibit or induce CYP3A4 (Peng *et al.*, 2002; O'Brien *et al.*, 2003; Bolton *et al.*, 2004;

Dutreix *et al*., 2004; van Erp *et al*., 2007). In contrast, the possibility that drug substrates or inhibitors of CYP2C8 may impair imatinib clearance does not appear to have been assessed extensively to date. A recent FDA report suggests there may be some potential for inhibition of the biotransformation of the CYP2C8 substrate paclitaxel by imatinib (FDA, 2001). This point is relevant in light of proposed trials of the efficacy of combined imatinib and paclitaxel for the treatment of papillary serous carcinoma of the uterus (NIH, 2010). Certainly, *in vitro* evidence suggests that this combination may be of value in decreasing the growth of ovarian cells in culture (Mundhenke *et al*., 2008). Thus, in individuals who express low levels of CYP3A4 in liver, CYP2C8 may be functionally important, which could lead to drug interactions with co-administered CYP2C8 inhibitors. The present findings that the CYP2C8 inhibitor quercetin was more likely to impair imatinib N-demethylation in livers containing high paclitaxel 6α-hydroxylation activity, relative to CYP3A activity, is consistent with this possibility. It is also feasible that genetic variation in CYP2C8 could also affect therapy by influencing the relative contribution of the enzyme to imatinib elimination (Bahadur *et al*., 2002).

There have been suggestions that other CYPs may contribute to imatinib N-demethylation in human liver. Using cDNA-expressed systems, it has been proposed that the polymorphic CYP2D6 may contribute to the activity (van Erp *et al*., 2007) and the manufacturer's literature reports that imatinib may be a substrate or inhibitor of several CYPs (FDA, 2006), but roles for CYPs other than CYP2C8 and CYPs 3A were not evident from the present study. The reasons for this are unclear, but the present study adopted a coordinated series of experimental approaches to test the involvement of several CYPs in imatinib N-demethylation. For example, in the case of CYP2D6, it is noteworthy that imatinib N-demethylation in human liver microsomes was not correlated with the CYP2D6-mediated O-demethylation of dextromethorphan, and was refractory to the CYP2D6 inhibitors quinidine and timolol. Moreover, it was reported recently that inhibitory effects of imatinib co-administration on the pharmacokinetics of metoprolol, which is metabolized in part by CYP2D6, were unrelated to CYP2D6 status (Wang *et al*., 2008). Considered together, there appears to be little evidence of a major role for CYP2D6 in imatinib clearance *in vivo*.

The dimensions of the substrate-binding cavities of CYPs 3A4 and 2C8 have been derived from crystal structures and have been reported recently. Both enzymes have large active sites of ~1400 $Å^3$, which is consistent with their abilities to accommodate large bulky substrates that are not oxidized by other CYPs (Schoch *et al*., 2004; Yano *et al*., 2004). The structure of CYP3A4 is more open than CYP2C8 in the region adjacent to the CYP haem moiety, at which oxygen activation occurs during catalysis (Yano *et al*., 2004); this may account for the wider substrate specificity of CYP3A4 compared with CYP2C8. Pharmacophoric models for substrates of both CYP3A4 and CYP2C8 have also been described (Ekins *et al*., 1999; Ridderstrom *et al*., 2001; Melet *et al*., 2004). These models have identified structural features within typical substrates that promote interactions with the enzymes, including hydrophobic/aromatic stretches and polar/hydrogen-binding moieties within the molecules that facilitate interactions with particular active site residues. In the present study, two of these pharmacophore models were used in an attempt to account for the roles of CYPs 2C8 and 3A4 in imatinib oxidation. Nineteen low-energy conformers of imatinib were generated and overlayed with the pharmacophore models for CYP2C8 and CYP3A4 of Melet *et al*. (2004) and Ekins *et al*. (1999) respectively. The conformations of imatinib when fitted to these models are shown in Figure 6; for purposes of clarity, imatinib only is shown in the figure.

Imatinib was superimposed on the proposed CYP2C8 pharmacophore and exhibited significant overlap with the polar residue (blue sphere) and the hydrophobic or ring region (green sphere). The reported pharmacophore model for CYP3A4 fitted the structural features of imatinib less well, with the possible exception of the carbonyl H-bond acceptor. Considered together, the CYP2C8 pharmacophoric model accommodates imatinib more completely than the corresponding CYP3A4 model. There are several factors that may underlie this situation. From the present study, CYP2C8 has emerged as a high-affinity catalyst towards imatinib oxidation relative to the lower-affinity CYP3A4; this may account for the superior overlap of the imatinib structure with those of other CYP2C8 substrates. Moreover, at least two binding modes have been described for CYP3A4 on the basis of kinetic and inhibitor studies (Shou *et al*., 1999). The relationship of imatinib binding to the active regions of the enzyme remains to be clarified. Considered together, CYP3A4 is a versatile catalyst that has a more accessible active site than CYP2C8, and contributes to the biotransformation of many drugs. In the case of imatinib, it emerges as an enzyme of lower affinity, but greater capacity than CYP2C8.

In summary, the present investigation has found that CYPs 3A and 2C8 participate in the hepatic formation of N-demethylimatinib, an active metabolite of the parent drug. This is based on findings with cDNA-expressed CYPs, correlation

approaches that revealed relationships between imatinib N-demethylation and microsomal oxidation of CYP3A and CYP2C8 substrates and the inhibition of N-desmethylimatinib formation by CYP3A4- and CYP2C8-specific inhibitors. The participation of CYP2C8 and CYP3A in imatinib oxidation in human liver may account in part for the wide inter-patient variation in imatinib elimination that is observed during therapy with the drug.

Acknowledgements

This study was supported by a grant from the Cancer Council NSW and SC was the recipient of a fellowship from the Swiss National Science Foundation. Imatinib mesylate, N-desmethylimatinib and imatinib-d8 were generous gifts from Novartis, and bupropion hydrochloride and hydroxybupropion were provided by GlaxoSmithKline. The assistance of Tina Gillani and Sussan Ghassabian in the determination of imatinib f_u is greatfully acknowledged.

Conflict of interest

The authors state no conflict of interest.

References

Alexander SPH, Mathie A, Peters JA (2009). *Guide to Receptors and Channels (GRAC)*, 4th edn. Br J Pharmacol 158 (Suppl. 1): S1–S254.

Apperley JF (2007). Part I: mechanisms of resistance to imatinib in chronic myeloid leukaemia. Lancet Oncol 8: 1018–1029.

Ayoub WS, Geller SA, Tran T, Martin P, Vierling JM, Poordad FF (2005). Imatinib (Gleevec)-induced hepatotoxicity. J Clin Gastroenterol 39: 75–77.

Bahadur N, Leathart JB, Mutch E, Steimel-Crespi D, Dunn SA, Gilissen R *et al.* (2002). CYP2C8 polymorphisms in Caucasians and their relationship with paclitaxel 6α-hydroxylase activity in human liver microsomes. Biochem Pharmacol 64: 1579–1589.

Blasdel C, Egorin MJ, Lagattuta TF, Druker BJ, Deininger MW (2007). Therapeutic drug monitoring in CML patients on imatinib. Blood 110: 1699–1701.

Bolton AE, Peng B, Hubert M, Krebs-Brown A, Capdeville R, Kellera U *et al.* (2004). Effect of rifampicin on the pharmacokinetics of imatinib mesylate (Gleevec, STI571) in healthy subjects. Cancer Chemother Pharmacol 53: 102–106.

Crespi CL, Penman BW (1997). Use of cDNA-expressed human cytochrome P450 enzymes to study potential drug–drug interactions. Adv Pharmacol 43: 171–188.

Deininger M (2008). Resistance and relapse with imatinib in CML: causes and consequences. J Natl Compr Canc Netw 6 (Suppl. 2):S11–S21.

Delbaldo C, Chatelut E, Deroussent MRA, Sronie-Vivien S, Jambu A, Berthaud P *et al.* (2006). Pharmacokinetic–pharmacodynamic relationships of imatinib and its main metabolite in patients with advanced gastrointestinal stromal tumors. Clin Cancer Res 12: 6073–6078.

Demetri GD, von Mehren M, Blanke CD, Van den Abbeele AD, Eisenberg B, Roberts PJ *et al.* (2002). Efficacy and safety of imatinib mesylate in advanced gastrointestinal stromal tumors. N Engl J Med 347: 472–480.

Druker BJ, Tamura S, Buchdunger E, Ohno S, Segal GM, Fanning S *et al.* (1996). Effects of a selective inhibitor of the Abl tyrosine kinase on the growth of Bcr-Abl positive cells. Nat Med 2: 561–566.

Dutreix C, Peng B, Mehring G, Hayes M, Capdeville R, Pokorny R *et al.* (2004). Pharmacokinetic interaction between ketoconazole and imatinib mesylate (glivec) in healthy subjects. Cancer Chemother Pharmacol 54: 290–294.

Ekins S, Bravi G, Wikel JH, Wrighton SA (1999). Three-dimensional-quantitative structure activity relationship analysis of cytochrome P-450 3A4 substrates. J Pharmacol Exp Ther 291: 424–433.

van Erp NP, Gelderblom H, Karlsson MO, Li J, Zhao M, Ouwerkerk J *et al.* (2007). Influence of CYP3A4 inhibition on the steady-state pharmacokinetics of imatinib. Clin Cancer Res 13: 7394–7400.

FDA (US Food and Drug Administration) (2001). Gleevec: drug interactions, caution advised. Available at: http://www.fda.gov/cder/foi/nda/2001/21335Gleevec.htm (accessed 8/3/2008).

FDA (US Food and Drug Administration) (2006).Gleevec: prescribing information. Available at:http://www.fda.gov/Drugs/DrugSafety/PostmarketDrugSafetyInformationforPatientsandProviders/ucm110502.htm (accessed 6/5/2010).

Gardner ER, Burger H, van Schaik RH, van Oosterom AT, de Bruijin EA, Guetens G *et al.* (2006). Association of enzyme and transporter genotypes with the pharmacokinetics of imatinib. Clin Pharmacol Ther 80: 192–201.

Goldman JM (2007). How I treat chronic myeloid leukemia in the imatinib era. Blood 110: 2828–2837.

Guilhot F (2004). Indications for imatinib mesylate therapy and clinical management. Oncologist 9: 271–281.

Gurney H, Wong M, Balleine R, McLachlan AJ, Hoskins JM, Wilcken N *et al.* (2007). Imatinib disposition and ABCB1 (MDR1 P-glycoprotein) genotype. Clin Pharmacol Ther 82: 33–40.

Kerkela R, Grazette L, Yacobi R, Iliescu C, Patten R, Beahm C *et al.* (2006). Cardiotoxicity of the cancer therapeutic agent imatinib mesylate. Nat Med 12: 908–916.

Loboz K, Gross AS, Ray J, McLachlan AJ (2005). HPLC assay for bupropion and its major metabolites in human plasma. J Chromatogr 823: 115–121.

Lowry OH, Rosebrough NJ, Farr AL, Randall RJ (1951). Protein measurement with the folin phenol reagent. J Biol Chem 193: 265–275.

Melet A, Marques-Soares C, Schoch GA, Macherey AC, Jaouen M, Dansette PM *et al*. (2004). Analysis of human cytochrome P450 2C8 substrate specificity using a substrate pharmacophore and site-directed mutants. Biochemistry 43: 15379–15392.

Miles JS, McLaren AW, Forrester LM, Glancey MJ, Lang MA, Wolf CR (1990). Identification of the human liver cytochrome P-450 responsible for coumarin 7-hydroxylase activity. Biochem J 267: 365–371.

Mundhenke C, Weigel MT, Sturner KH, Roesel F, Meinhold-Heerlein I, Bauerschlag DO *et al*. (2008). Novel treatment of ovarian cancer cell lines with imatinib mesylate combined with paclitaxel and carboplatin leads to receptor-mediated antiproliferative effects. J Cancer Res Clin Oncol 134: 1397–1405.

Murray M (1992). Metabolite intermediate complexation of microsomal cytochrome P450 2C11 in male rat liver by nortriptyline. Mol Pharmacol 42: 931–938.

Murray M, Wilkinson CF, Dube CE (1983). Effects of dihydrosafrole on cytochromes P-450 and drug oxidation in hepatic microsomes from control and induced rats. Toxicol Appl Pharmacol 68: 66–76.

Murray M, Butler AM, Stupans I (1994). Competitive inhibition of human liver microsomal P450 3A-dependent steroid 6β-hydroxylation activity by cyclophosphamide and ifosfamide *in vitro*. J Pharmacol Exp Ther 270: 645–649.

NIH (US National Institutes of Health) (2010). Gleevec/taxol for patients with uterine papillary serous carcinoma. Available at: http://www.clinicaltrials.gov/ct2/show/NCT00506779?term=paclitaxel+and+gleevec&rank=3 (accessed 6/5/2010).

O'Brien SG, Meinhardt P, Bond E, Beck J, Peng B, Dutreix C *et al*. (2003). Effects of imatinib mesylate (STI571, Glivec) on the pharmacokinetics of simvastatin, a cytochrome P450 3A4 substrate, in patients with chronic myeloid leukemia. Br J Cancer 89: 1855–1859.

Peng B, Knight H, Riviere GJ, Rouilly M, Brown AK, Lane A *et al*. (2002). Pharmacokinetic interaction between Gleevec (imatinib) and cyclosporin. Blood 100: 433b–434b.

Peng B, Lloyd P, Schran H (2005). Clinical pharmacokinetics of imatinib. Clin Pharmacokinet 44: 879–893.

Picard S, Titier K, Etienne G, Teilhet E, Ducint D, Bernard MA *et al*. (2007). Trough imatinib plasma levels are associated with both cytogenetic and molecular responses to standard-dose imatinib in chronic myeloid leukemia. Blood 109: 3496–3499.

Ridderstrom M, Zamora I, Fjellstrom O, Andersson TB (2001). Analysis of selective regions in the active sites of human cytochromes P450, 2C8, 2C9, 2C18, and 2C19 homology models using GRID/CPCA. J Med Chem 44: 4072–4081.

Schoch GA, Yano JK, Wester MR, Griffin KJ, Stout CD, Johnson EF (2004). Structure of human microsomal cytochrome P450 2C8. Evidence for a peripheral fatty acid binding site. J Biol Chem 279: 9497–9503.

Shimada T, Yamazaki H, Mimura M, Inui Y, Guengerich FP (1994). Interindividual variation in human liver cytochrome P-450 enzymes involved in the oxidation of drugs, carcinogens and toxic chemicals: studies with liver microsomes of 30 Japanese and 30 Caucasians. J Pharmacol Exp Ther 270: 414–423.

Shou M, Mei Q, Ettore MW Jr, Dai R, Baillee TA, Rushmore TH (1999). Sigmoidal kinetic model for two co-operative substrate-binding sites in a cytochrome P450 3A4 active site: an example of the metabolism of diazepam and its derivatives. Biochem J 340: 845–853.

Solassol I, Bressolle F, Philibert I, Charasson V, Astre C, Pinguet F (2006). Liquid chromatography–electrospray mass spectrometry determination of imatinib and its main metabolite, N-desmethylimatinib in human plasma. J Liq Chromatogr Relat Technol 29: 2957–2974.

Su GM, Fiala-Beer E, Weber J, Jahn D, Robertson GR, Murray M (2005). Pretranslational upregulation of microsomal CYP4A in rat liver by intake of a high-sucrose, lipid-devoid diet containing orotic acid. Biochem Pharmacol 69: 709–717.

Sueyoshi T, Negishi M (2001). Phenobarbital response elements of cytochrome P450 genes and nuclear receptors. Annu Rev Pharmacol Toxicol 41: 123–143.

Vaclavikova R, Soucek P, Svobodova L, Anzenbacher P, Simek P, Guengerich FP *et al*. (2003). Different *in vitro* metabolism of paclitaxel and docetaxel in humans, rats, pigs and minipigs. Drug Metab Dispos 32: 666–674.

Wang Y, Zhou L, Dutreix C, Leroy E, Yin Q, Sethuraman V *et al*. (2008). Effects of imatinib (Glivec) on the pharmacokinetics of metoprolol, a CYP2D6 substrate, in Chinese patients with chronic myelogenous leulaemia. Br J Clin Pharmacol 65: 885–892.

Yano JK, Wester MR, Schoch GA, Griffin KJ, Stout CD, Johnson EF (2004). The structure of human microsomal cytochrome P450 3A4 determined by X-ray crystallography to 2.05-A resolution. J Biol Chem 279: 38091–38094.

Zhang WV, Ramzan I, Murray M (2007). Impaired microsomal oxidation of the atypical antipsychotic agent clozapine in hepatic steatosis. J Pharmacol Exp Ther 322: 770–777.

Zhang WV, d'Esposito F, Edwards RJ, Ramzan I, Murray M (2008). Inter-individual variation in relative CYP1A2/3A4 phenotype influences susceptibility of clozapine oxidation to CYP-specific inhibition in human hepatic microsomes. Drug Metab Dispos 36: 2547–2555.